Journal of the Ceramic Society of Japan 117 [7] 836-841 2009 Paper

Relation between functional properties of alumina-based nanocomposites and locations of dispersed particles

Yoshitaka NISHIMURA,[*,,†] Kenichiro AIKAWA,[*] Seong-Min CHOI,[**] Shinobu HASHIMOTO[*] and Yuji IWAMOTO[*]**

[*]Nagoya Institute of Technology, Gokiso-cho, Showa-ku, Nagoya, Aichi 466−8555
[**]Fuji Electric Device Technology, 4−18−1, Tsukama, Matsumoto-shi, Nagano 390−0821

We previously proposed the toughening and strengthening mechanisms of alumina-based nanocomposites on the basis of dislocation activities, assuming that nano-sized particles were embedded within the alumina grains. In this research, we fabricated both intragranular dominant and intergranular dominant nanocomposites of alumina/nickel(Ni) system. In order to fabricate intragranular dominant nanocomposites, γ-alumina powder with many nanopores was used as a starting material through a soaking method. Intergranular dominant nanocomposites were prepared using α-alumina powder as a starting material. Monolithic alumina samples were also sintered for comparison. Mechanical, thermal, and electrical properties were estimated for those specimens. The results showed that the intragranular nanocomposites had a higher mechanical strength and fracture toughness than the intergranular nanocomposites. The values of thermal expansion and thermal conductivity were slightly high in the intragranular nanocomposites compared to the intergranular one. The intergranular nanocomposites indicated a low dielectric breakdown voltage. Relations between the functional properties of the nanocomposites and the location of the dispersed Ni particles were discussed based on dislocation activities and the percolation model.

Key-words : Nanocomposites, Alumina, Nickel, Thermal expansion, Thermal conductivity, Dielectric constant, Breakdown voltage

[Received March 16, 2009; Accepted May 21, 2009]

1. Introduction

Ceramics have excellent insulation properties. Meanwhile, it is widely known that ceramics are also hard, mechanically brittle, low thermal expansion coefficient and low thermal conductivity. Much research has been conducted to improve the mechanical characteristics of ceramics, including that of aiming to improve the fracture toughness on the bridging effect obtained when heterogeneous particles are distributed over ceramics.[1)–3)] Regarding thermal characteristics, an improved thermal expansion coefficient and thermal conductivity can be obtained by creating a ceramic–metal composite.[4),5)] However, in a composite created by adding metal particles, since the characteristics of metal is used to obtain the thermal expansion coefficient and thermal conductivity closer to those of metallic materials. There is lack of study of the insulation properties of ceramic–metal composites.

Following the development of nanocomposites created by adding nanoparticles, a method of obtaining new characteristics was proposed. Ceramic-based nanocomposites were originally proposed by Niihara.[6)]

In our previous report in which a nanocomposite was created by adding Ni particles to γ-alumina, the amount of added Ni influenced the characteristics of the nanocomposite matrix.[7)] The position of Ni particle in alumina matrix changed with the quantity of Ni. Agglomerated Ni particles existed mostly along alumina grain boundaries especially for 5 vol% Ni. However, the effect of the position of second phase particles on the macroscopic properties of nanocomposites has yet to be clarified, while in composites, second phase particles affect the characteristics of the matrix.

The aim of this study is to clarify the effects of the location of the second phase particles on characteristics of nanocomposites. We fabricate intragranular dominant nanocomposites using γ-alumina powder with many nanopores as a starting material (called γ-alumina composites) and intergranular dominant nanocomposites using α-alumina powder as a starting material (called α-alumina composites). Also, we control the amount of Ni, estimate the mechanical, thermal, and electrical characteristics for each material, and discuss the effects of the locations of the second phase particles on the characteristics.

2. Experimental procedure

2.1 Starting materials

In this research, samples were prepared by the Pulsed Electric Current Sintering (PECS) method, using mixed powder created by the soaking method,[8)] in order to create a Ni dispersed alumina matrix nanocomposite. The two types of commercially available alumina, γ-alumina (AKP–G015, Sumitomo Chemical Co., purity: 99.99%, average coagulated particle diameter: 2.6 μm) and α-alumina (AKP–53, Sumitomo Chemical Co., average particle diameter: 0.3 μm), were used as starting material matrices. Ni nitrate (Kishida Reagents Chemicals, purity: 98.0%) was used as a starting material to obtain nanosized Ni, which formed a dispersion phase. When γ-alumina was used as a matrix, α-alumina was added by 10 mass% as a seed to improve the sinterability of alumina matrix, while Ni nitrate solution was prepared by adjusting the Ni content, so that the concentration becomes 1, 3, 5, and 10 vol% of the volume of alumina. Alumina, which was the matrix, was added to the Ni nitride solution, which was then agitated with a stirrer for 30 min, vacuuming was performed for 30 min for depressurization, and the Ni

† Corresponding author: Y. Nishimura; E-mail: nishimura-yoshitaka-m@fujielectric.co.jp

nitride solution was taken in between coagulated alumina particles. Drying was then performed in a dryer set at 70°C for 48 h, and the mixture was crushed in an alumina mortar. The obtained powder was maintained at 500°C in an atmosphere for 2 h for temporary sintering. Furthermore, the oxidized Ni obtained as a result of temporary sintering was reduced into Ni, which was subsequently maintained at 800°C in a hydrogen atmosphere (100%) for 2 h to obtain an alumina/Ni powder mixture. Finally, α-alumina was added by 10 mass% as a seed to the powder mixture, which was finally mixed in a ball mill and dried for 24 h.

2.2 Preparation of sintered samples

A carbon die (diameter: 20 mm) was filled with an alumina/Ni powder mix, and sintering was performed by the pulse electric current sintering (PECS) method in a vacuum, with the sintering temperature set at 1350°C and the sintering pressure at 30 MPa. To check the phase transformation of alumina and oxidation of Ni metal during the sintering process, sintering was performed with temperatures set at 1000°C, 1100°C, and 1200°C respectively, and the pressure at 30 MPa.

2.3 Observation of the microstructure

Using samples subjected to a three-point bending strength test, the fracture surface of alumina-Ni nanocomposite was observed under a scanning electron microscope (SEM:JSM–5200, JEOL Ltd.), and its fracture mode examined. In addition, the post-sintering dispersion status of nanosize Ni particles was observed under a transmission electron microscope (TEM:JEM0–3010, JEOL Ltd.) in order to examine its relation with various characteristics, while the behavior of Ni particles when sintering was performed at 1000°C under 30 MPa was also observed.

2.4 Characterization

The bulk density of the sintered samples was measured by the Archimedes method. The phase transformation of alumina and oxidation of Ni particles of the mixed powder were checked at each temperature using the X-ray diffraction (XRD) method. Furthermore, post-sintering Ni existing in the samples was quantified by fluorescent X-ray analysis (XRF).

A $2 \times 2 \times 10$ mm^3 specimen was cut out of a sintered sample, and its fracture strength measured using a three-point fracture strength test(Autograph; AGS–5kND, Shimadzu Co.). The fracture strength test was carried with the span size set at 8 mm and the crosshead speed at 0.5 mm/min. To measure the fracture toughness, a $2 \times 2 \times 10$ mm^3 specimen was also cut out as in the case of fracture strength measurement, a V-shaped notch of depth 1 mm and end curvature radius of 20 μm was processed at the center of the specimen, and a fracture toughness test was used by the SEVNB method.[8] The fracture toughness test was carried with the span size set at 8 mm and the crosshead speed at 0.5 mm/min. The fracture toughness was calculated by the equation presented by Wakai et al.,[9] using the results obtained.

Thermal expansion was measured with the specimens in disk shape with thickness of 10 mm and diameter of 5 mm was used for the thermo mechanical analyzer (TMA–50H, Shimadzu Co.)(JIS R 1618). The measurement temperature is from room temperature to 300°C in Ar atmosphere.

The specific heat and thermal diffusivity at room temperature were measured by the laser flash method (JIS R 1611) in order to determine the thermal conductivity. A laser flash device (TC–7000, Optronics Co., Ltd.) was used for the measurement, and specimens in disk shape with thickness of 1 mm and diameter of 10 mm were used. To stabilize the laser absorption on the surface of the specimens in specific heat measurement, glassy carbon was attached to them, and to measure thermal diffusivity, the sample was performed by spraying carbon onto both sides of the specimens.

The dielectric breakdown voltage was measured as electric characteristics. To test these properties, disk-shaped specimens with thickness of 1 mm and diameter of 10 mm were cut out and electrodes were attached to both faces of these specimens. In the dielectric strength voltage test, AC voltage was applied to both sides of the disk-shaped specimens at a voltage increase rate of 100 V/s, and the voltage at dielectric breakdown was measured to calculate the resistance to dielectric breakdown.

3. Results and discussion

3.1 The effect of starting material

It is likely that a starting material had a significant effect on the position or existence of Ni in the alumina matrix. Based on the assumption that the difference between the phase transformation temperature from γ-alumina to α-alumina and that of the start of sintering of α-alumina in the sintering process had an effect on the existence of Ni nanoparticles within alumina particles when γ-alumina was used, the temperature of the phase transformation was examined using the PECS method. **Figure 1** shows the results of X-ray diffraction analysis of γ-alumina/1vol%Ni nanocomposite powder and samples sintered at 1000, 1100, and 1200°C respectively. In powder, γ-alumina and seed α-alumina are seen. At 1000°C, γ-alumina is found to exist, but the peak of α-alumina is found to be slightly larger than that of the powder. At 1100°C, γ-alumina had completely transformed into α-alumina.

Figure 2 shows the result of TEM and Energy Dispersive X-ray Spectroscopy (EDX) of samples sintered at 1000°C and 30 MPa, while Fig. 2(a) shows that Ni particles had been dispersed within columnar γ-alumina and its aggregate. Figure 2(b) shows that phase transformation occurred to α-alumina partially. The results of TEM in (b) and EDX in (c) show that Ni existed within the alumina particles, which had been made into α-type. In pressureless sintering, the phase transformation from γ-alumina into α-alumina is known to start at approximately 1200°C. If sintering is performed by the PECS method, the sintering of α-alumina will commence at approximately 900°C. When γ-alumina is used as a starting material, phase transformation from γ-alumina to α-alumina occurs at 1100°C. In general, when grain growth speed was low the dispersed particles moved to grain-boundary, under the opposite case, the dispersed particles were left in the grain. In this case, the temperature of the phase transformation was

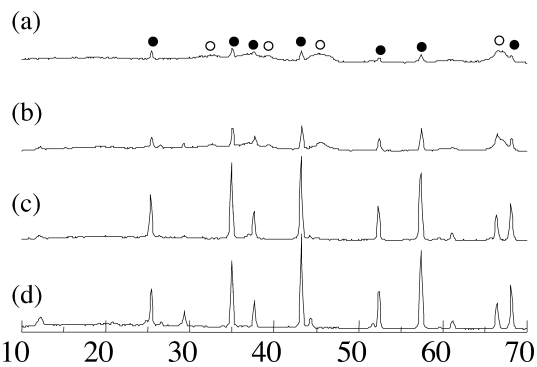

Fig. 1. XRD patterns of alumina/1vol%Ni nanocomposite. (a) powder, (b) 1000°C, (c) 1100°C, (d) 1200°C. ●α-alumina, ○γ-alumina.

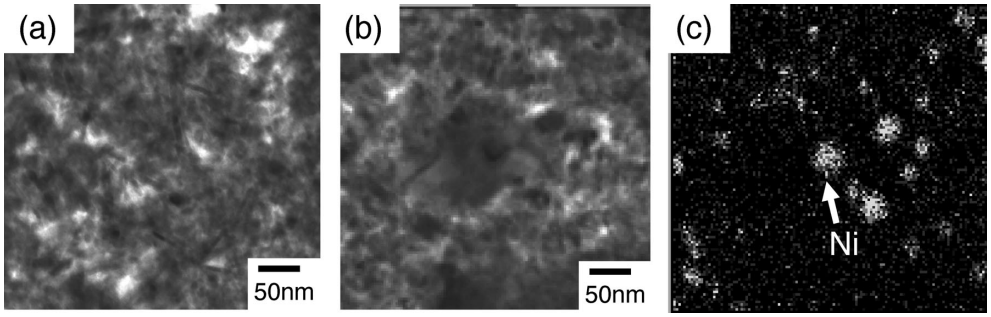

Fig. 2. TEM and EDX photographs of alumina/1vol% Ni nanocomposites sintered at 1000°C by PECS method. (a) Ni particles within γ-alumina, (b) Phase transformation from γ-alumina to α-alumina, (c) EDX analysis of (b).

higher than the α-alumina sintering start temperature. Therefore Ni particles were left within alumina particles, because grain growth of alumina particles occurred rapidly. Based on the above, by using α-alumina as a starting material, Ni particles moved to alumina grain boundaries, because the sintering start temperature of α-alumina is lower than that of γ-alumina.

3.2 Mechanical properties (bulk density, fracture strength, and fracture toughness)

Table 1 shows the Ni contents in several samples. When the samples measured using fluorescent X-rays were analyzed, the Ni content detected was almost the same as the amount added to the mixture. **Table 2** shows the results of measurement of the bulk density, fracture strength, and fracture toughness. The monolithic alumina and 1 vol% Ni added γ-alumina and α-alumina were sintered at 1350°C under 30 MPa. The bulk density of 1 vol% Ni samples was found to be almost equivalent to that of monolithic alumina, while the relative density of all the alumina matrix nanocomposites created was 99% or higher, which indicated that the substance obtained was highly dense with almost no pores. The fracture strength of the γ-alumina/1vol%Ni sample was measured by a 3-point fracture strength test at 900 MPa. On the other hand, the α-alumina/1vol%Ni sample did not demonstrate improved strength compared with monolithic alumina. The fracture toughness of γ-alumina/1vol%Ni sample measured by the SEVNB method was higher than that of monolithic alumina, whereas no improvement of fracture toughness was observed in the α-alumina/1vol%Ni sample. To examine the effect of the position of existence of Ni particles in alumina matrix nanocomposites on various ceramics characteristics, nanocomposite with Ni added was subjected to the fracture strength test, and the microstructure of the fracture surface was subsequently observed under an SEM to examine the fracture mode. The dispersion status of the Ni particles in the sintered body was also observed under a TEM. **Figure 3** shows SEM photographs of the fracture surface of samples prepared using α-alumina (a) and γ-alumina (b) as a matrix, respectively. The transgranular fracture mode was mainly found with γ-alumina, whereas with α-alumina, the intergranular fracture mode was mainly found although a transgranular fracture was also partially in evidence. **Figure 4** shows TEM photographs showing black Ni particles. The Ni particle size of both samples fell within the 100 to 300 nm range. In the sample using α-alumina (a), Ni particles were found mainly at the grain boundaries, whereas in the γ-alumina/1vol%Ni sample (b), Ni particles were found to exist within matrix particles, and the dislocation was found to occur around Ni particles. As a result, we consider that with γ-alumina/1vol%Ni sample, Ni particles dispersed

Table 1. Ni Contents in Several Samples

Ni contents	α-alumina	γ-alumina
1 vol%	1.2	1.3
3 vol%	3.1	3.2
5 vol%	5.1	4.9

Table 2. Mechanical Properties of Alumina/Nickel Nanocomposites

	Bulk Density	Fracture Strength	Fracture Toughness
	g/cc^3	MPa	MPa·m$^{1/2}$
alumina	3.9	757	4.00
α-alumina 1vol%Ni	3.9	730	3.43
γ-alumina 1vol%Ni	3.9	900	4.86

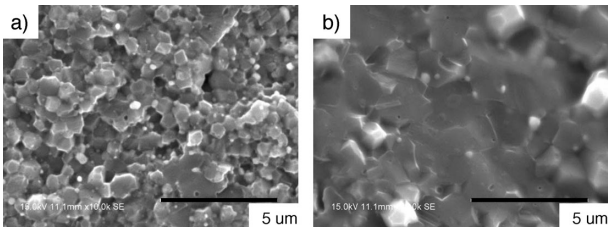

Fig. 3. SEM photographs of fracture surface of alumina/Ni nanocomposites sintered at 1350°C under 30 MPa by PECS method. (a) α-alumina/1vol% Ni, (b) γ-alumina/1vol%Ni.

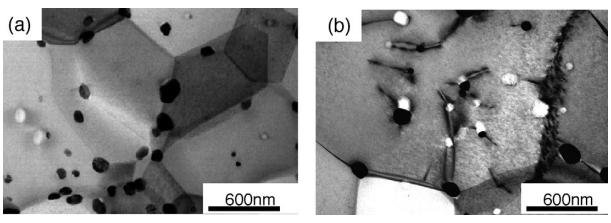

Fig. 4. TEM photographs of alumina/Ni nanocomposites sintered at 1350°C under 30 MPa by PECS method. (a) α-alumina/1vol% Ni, (b) γ-alumina/1vol%Ni.

within alumina particles caused the dislocation to occur. The dislocations within matrix could improve the fracture strength and fracture toughness because the residual stress in alumina decreased and the frontal process zone size increased.[10)]

On the other hand, the fracture strength and toughness of the α-alumina/1vol%Ni sample were approximately equivalent to those of monolithic alumina, due to the minute amount of Ni existing within the matrix particles compared with the volume of γ-alumina. Based on the results described above, we conclude that the existence of nanoparticles within the alumina matrix is very effective for improving both strength and toughness.

3.3 Thermal properties (thermal conductivity, thermal expansion coefficient)

When ceramics are used for insulated circuit boards, their thermal conductivity should preferably be maximized, because they constitute a means of heat dissipation. In addition, to ensure reliability, it is desirable that the thermal expansion coefficient be as close to that of copper, namely the circuit material, as possible. With these in mind, the thermal properties of ceramics, vital when they are used as insulated circuit board materials, were examined.

Figure 5 shows the relation between the Ni content and the thermal expansion. The broken line in the figure represents the upper limit of the rule of mixture (Voigt rule). The γ-alumina/1vol%Ni sample saw the thermal expansion coefficient compared with monolithic alumina, slightly exceeding the upper limit of the rule of mixture. Otherwise, the α-alumina/1vol%Ni sample demonstrated a decrease in the thermal expansion coefficient. Based on this, the position of the existence of Ni is likely to have affected the thermal expansion coefficient. Local stress caused by the difference in the thermal expansion coefficient between the matrix and the dispersion phase can be expressed by the following equation, using Selsing's model:[11)]

$$\sigma = \frac{(\alpha_m - \alpha_p)\times\Delta T}{\frac{1+\nu_m}{2E_m}+\frac{1-2\nu_p}{E_p}} \quad (1)$$

where,

α: Thermal expansion coefficient
ν: Poisson's ratio
E: Young's modulus of elasticity
ΔT: Temperature difference in the cooling process
m: Matrix, and
p: Dispersion phase value

The compressive stress generated around dispersed Ni particles in the alumina-Ni system is calculated to be approximately 1900 MPa by Eq. (1), assuming that the temperature difference ΔT is 1330°C.

In those results, we suggest that relationship between residual stress and position of Ni particles as shown in **Fig. 6**. A sintered monolithic alumina (Fig. 6(a)) will have residual stresses in grains. If Ni exists within alumina particles (Fig. 6(b)), compressive stress is generated on the joint interface between alumina and Ni, resulting in dislocation. Consequently, the sintering residual stress of alumina decreased, while the thermal expansion coefficient increases, reaching a value close to the coefficient of the linear expansion of sapphire (parallel to *C*-axis: 7.7×10^{-6}/K (40 to 400°C)). On the other hand, with the α-alumina/1vol%Ni sample, since Ni existed within the alumina grain boundaries (Fig. 6(c)), the residual stress of alumina particles increased during sintering, the thermal expansion coefficient decreased.

Figure 7 shows the change in thermal conductivity due to the addition of Ni. Generally, the thermal conductivity of composites is determined by the thermal conductivity, volume fraction, and status of interface of composites. Hasselman et al. presented a theoretical Eq. (1) to calculate the thermal conductivity of particle-dispersed composites consisting of 2 phases.[11)]

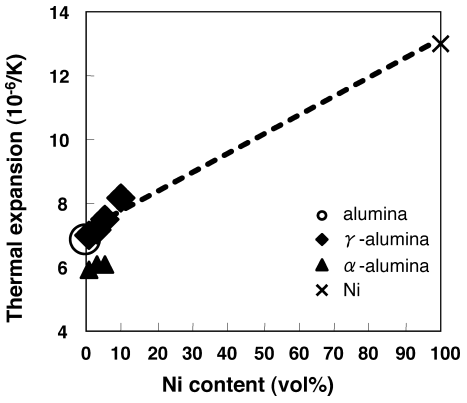

Fig. 5. Relation between Ni content and thermal expansion of monolithic alumina and alumina/Ni nanocomposites.

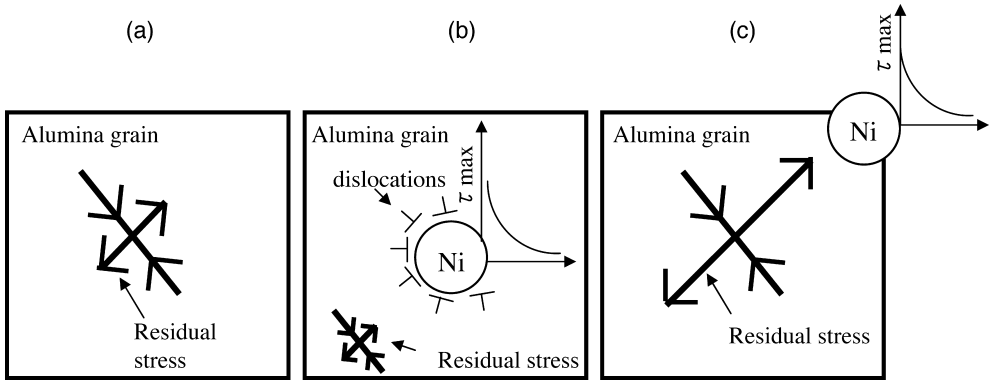

Fig. 6. Relation between residual stress and position of Ni particles. (a) monolithic alumina, (b) Ni exists within alumina grain, (c) Ni existed within the alumina grain boundaries.

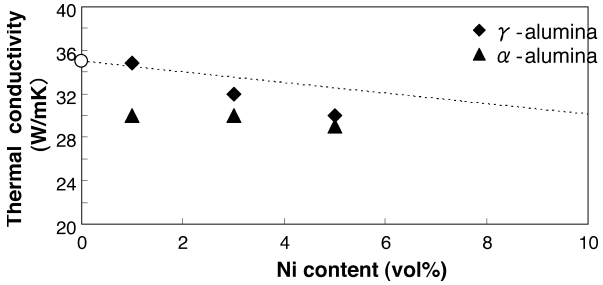

Fig. 7. Relation between Ni content and thermal conductivity of alumina/Ni nanocomposites.

$$K = K_m \frac{2(\frac{K_d}{K_m} - \frac{K_d}{ah_c} - 1)V_d + \frac{K_d}{K_m} + 2\frac{K_d}{ah_c} + 2}{(1 - \frac{K_d}{K_m} + \frac{K_d}{ah_c})V_d + \frac{K_d}{K_m} + 2\frac{K_d}{ah_c} + 2} \quad (1)$$

where,

K_m: Thermal conductivity of the matrix
K_d: Thermal conductivity of the dispersion phase
V_d: Volume fraction of the dispersion phase
a: Particle diameter, and
h_c: Coefficient concerning the thermal conduction on the interface

The size effect of the Ni particle diameter on thermal conductivity was examined within the Ni content range of 1 to 5 vol%. The size of the Ni particle diameter in 1 to 5 vol% ranged from 100 to 500 nm. When the Ni particle diameter increased from 100 to 500 nm, the difference in thermal conductivity was calculated to be as small as 0.3 W/m·K using the above equation, which indicated that the effect of the particle diameter on thermal conductivity was small. The broken line in the figure represents the relation between Ni content and thermal conductivity when the Ni particle diameter is 100 nm, and h_c is 3.5×10^7. The γ-alumina/1vol%Ni sample slightly exceeded the theoretical thermal conductivity by Hasselman. However, with the increase in Ni content, the value decreased to below the theoretical conductivity by Hasselman. The thermal conductivity of the α-alumina/1vol%Ni sample was found to be lower than that of monolithic alumina by approximately 17%, and lower than the theoretical thermal conductivity by Hasselman. **Table 3** shows the results of measurement of thermal diffusivity and specific heat of the γ-alumina/1vol%Ni and α-alumina/1vol%Ni samples. The specific heat of both samples was found to be approximately equivalent to that of monolithic alumina. The thermal diffusivity of the γ-alumina/1vol%Ni sample was higher than that of monolithic alumina, whereas that of the α-alumina/1vol%Ni sample was lower than that of monolithic alumina. The above results indicate that the difference in thermal conductivity between the γ-alumina/1vol%Ni and α-alumina/1vol%Ni samples is affected by thermal diffusivity. The major factor affecting the thermal conduction of ceramics is phonon diffusion due to lattice vibration. Increased dislocation in crystals prevents the lattice from producing harmonic oscillation, thus resulting in attenuation. Consequently, phonons are scattered and thermal conductivity declines significantly.[12] Several studies have reported that increased residual stress on the lattice causes strain, thus decreasing thermal conductivity.[13] With the α-alumina/1vol%Ni sample, the residual stress on Ni existing in alumina grain-boundaries (lattice strain) caused phonon scattering attributable to lattice vibration, thus decreasing the thermal conductivity.

Table 3. Thermal Properties of Monolithic Alumina and Alumina Nanocomposites

sample	Specific Heat	Thermal Diffusivity
	$\times 10^3$ J/kgK	$\times 10^{-6}$ m^2/s
alumina	0.77	12.21
α-alumina 1vol%Ni	0.76	9.76
γ-alumina 1vol%Ni	0.74	13.02

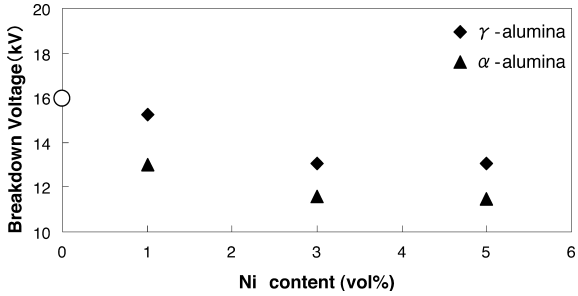

Fig. 8. Relation between Ni content and breakdown voltage of alumina/Ni nanocomposites.

Meanwhile, with the γ-alumina/1vol%Ni sample, despite the fact that dislocation occurred within alumina particles, the thermal conductivity remained unchanged. Therefore it is likely that the major reason for this is the fact that the existence of Ni within alumina particles decreased the residual stress within the alumina particles.

3.4 Electrical characteristics

Figure 8 shows the relation between the Ni content and breakdown voltage. The breakdown voltage of the γ-alumina/1vol%Ni sample was lower than that of monolithic alumina by 4%, whereas the breakdown voltage of the α-alumina/1vol%Ni sample was lower by approximately 19%.

A leak electric current is generated with an increase of the voltage that is applied to alumina matrix. The increase in leak electric current produces breakdown.[14),15)] The electrical characteristics of composites were examined based on the percolation phenomenon.[16)] The percolation threshold of materials with conductive materials added to its insulator varies depending on the parent phase particle/conductive particle diameter ratio. If conductive particles have a sufficiently small diameter compared with that of the parent phase, the critical volume decreases, and conductivity is attained when only a small amount of conductive substance is added. Consequently, the addition of sufficiently small nanosize Ni, even in trace amounts, may hinder efforts to maintain the insulation properties.[17)] Since the TEM observation result indicates that the ratio of the alumina particle diameter to the Ni particle diameter in the γ-alumina/1vol%Ni and α-alumina/1vol%Ni samples was approximately 15:1, there is sufficient potential for the withstand voltage to have decreased based on the percolation theory. The existence of Ni particles at the grain boundaries of the α-alumina/1vol%Ni sample decreased the withstand voltage based on the percolation theory. Based on the above, the position of the existence of Ni in alumina/nanosize Ni composites is considered to affect the breakdown voltage of ceramics. However, since Ni existed within alumina particles of the γ-alumina/1vol%Ni sample, the

percolation theory was not applicable, and the withstand voltage hardly decreased, thus ensuring approximately the same dielectric breakdown voltage as that of monolithic alumina.

4. Conclusion

The position of the existence of nanosize nickel (Ni) in alumina matrix was changed to examine the mechanical, thermal, and electrical characteristics of nanocomposites, and the following results were obtained:

(1) The Ni particle dispersion status in the microstructure of nanocomposites varied depending on the type of alumina used as a starting material. With the γ-alumina/1vol%Ni sample, Ni particles existed mainly within alumina particles, whereas with the α-alumina/1vol%Ni sample, Ni particles existed mainly at grain boundaries.

(2) The existence of Ni particles within alumina particles improved the mechanical characteristics (fracture strength and fracture toughness) compared with those of monolithic alumina. However, if Ni existed at grain boundaries, the mechanical characteristics remained unchanged, even if the particle size was the same.

(3) The existence of Ni particles within alumina particles also improved the thermal characteristics (thermal expansion and thermal conductivity coefficients) as in the case of mechanical characteristics. Meanwhile, the existence of Ni at grain boundaries decreased the thermal expansion coefficient to 6 ppm/K, and that of thermal conductivity to 30 W/m·K, from those of monolithic alumina.

(4) The existence of Ni particles within alumina particles decreased the breakdown voltage by 4%, whereas their existence at grain boundaries decreased it by 19%.

References

1) F. Erdogan and F. Joseph, *J. Am. Ceram. Soc*., **72**, 262 (1989).
2) V. Trergaard, *Int. J. Mech. Soc.*, **34**, 635 (1992).
3) F. Tamai and K. Hirano, *Trans of JSME Ser. A.*, **63**, 1172–1177 (1997).
4) C. Kawi, M. Miyanaga and J. J. Park, *J. Ceram. Soc. Japan*, **109**, 565–569 (2001).
5) A. P. Divecha, S. G. Fishman and S. D. Karmarkar, *J. Metals*, **9**, 12 (1981).
6) K. Niihara, *J. Ceram. Soc. Japan*, **99**, 974–981 (1991).
7) Y. Nishimura, K. Aikawa, S.-M. Choi, S. Hashimoto and H. Awaji, *J. Soc. Mater. Sci. Japan*, **57**, 1054–1060 (2008).
8) T. Matsunaga, U. Leela-Adison, Y. Kobayashi, S.-M. Choi and H. Awaji, *J. Ceram. Soc. Japan*, **113**, 123–125 (2005).
9) F. Wakai, S. Shuji and Y. Matsuo, *J. Ceram. Soc. Japan*, **93**, 479–480 (1985).
10) H. Awaji, Y. Nishimura, S.-M. Choi, Y. Takahashi and T. Goto, *J. Ceram. Soc. Japan*, **117**, 623–629 (2009).
11) D. P. H. Hasselman, K. Y. H. Donaldson and A. L. Geiger, *J. Am. Ceram. Soc.*, **75**, 3137–3140 (1992).
12) A. Kuibira, H. Nakata and A. Yamaguchi, *J. Ceram. Soc. Japan*, **113**, 611–615 (2005).
13) T. Sekino, T. Adachi, T. Nakayama, T. Kusunose and K. Niihara, *Mater. Integ*., **18**, 27–33 (2005).
14) M. Yoshimura and H. K. Bowen, *J. Am. Ceram. Soc.*, **64**, 404–410 (1981).
15) H. Murata, S. C. Choi, K. Kumoto and H. Yanagida, *J. Mater. Sci.*, **20**, 4507–4513 (1985).
16) K. Yoshida, *J. Soc. Mater. Sci. Japan*, **39**, 103–113 (1990).
17) T. Tomimura, T. Okamoto, S. Nakamura and A. Oshita, *Trans. IEE Japan*, **A123-A**, 76–81 (2003).